

Extended applications of electric cell-substrate impedance sensing for assessment of the structure–function of $\alpha 2\beta 1$ integrin

John H.T. Luong^{a,*}, Caide Xiao^a, Bernard Lachance^a, Š. Mircea Leabu^{b,c}, Xiaolan Li^{b,c}, Shashi Uniyal^{b,c}, Bosco M.C. Chan^{b,c}

^a Biotechnology Research Institute, National Research Council Canada, Montreal, Que., Canada H4P 2R2

^b Biotherapeutic Research Group, Robarts Research Institute, London, Ont., Canada N6A 5C1

^c Department of Microbiology and Immunology, The University of Western Ontario, London, Ont., Canada N6A 5C1

Received 16 January 2003; received in revised form 4 July 2003; accepted 15 September 2003

Abstract

Electric cell-substrate impedance sensing (ECIS) was applied to assess the structure–function of $\alpha 2\beta 1$ integrin, receptor for collagen and laminin. On collagen-coated gold electrodes, expression of this integrin on human rhabdomyosarcoma (RD) cells (RDX2C2) yielded a five-fold increase in resistance when compared with mock transfected RD (RDpF) cells (34.5 ± 5.2 versus $6.5 \pm 0.8 \Omega/\text{cell}$). An intermediate level of $16 \pm 2 \Omega/\text{cell}$ was measured upon expression of an $\alpha 2\beta 1$ mutant that lacked the $\alpha 2$ cytoplasmic domain (RDX2CO). On laminin, the resistance measured for RDX2C2 cells was also higher but only twice that of RDpF cells at 71 ± 4 and $37 \pm 4 \Omega/\text{cell}$, respectively. In comparison, RDX2CO cells ($38 \pm 4 \Omega/\text{cell}$), exhibiting no enhanced adhesive function, yielded a similar result to that of RDpF cells. On fibronectin, RDX2C2 and RDpF cells, exhibiting comparable levels of adhesion, were similar in resistance measurements at 85 ± 5 and $89 \pm 7 \Omega/\text{cell}$, respectively. It has been shown that deletion of $\alpha 2$ cytoplasmic domain results in dysregulated recruitment of the $\alpha 2\beta 1$ mutant to focal adhesion complexes that mediate binding of fibronectin. RDX2CO cells on fibronectin, exhibiting reduced adhesive function, was associated with noticeably lower resistance ($60 \pm 4 \Omega/\text{cell}$). Monitoring electroporation of the RD plasma membrane also indirectly validated cell attachment as reflected by the resistance measured. Results from this study demonstrated the potential of ECIS for study of the structure–function of $\beta 1$ integrin adhesion receptors.

© 2003 Elsevier B.V. All rights reserved.

Keywords: Impedance measurement; Cell Adhesion; Fibronectin; Laminin; Collagen; Human rhabdomyosarcoma cells

1. Introduction

Electric cell-substrate impedance sensing (ECIS) has been developed for real time measurements of the changing impedance properties of attached and spread cells that act as insulating particles on gold electrodes [1]. The technique involves application of a small ac current (1 μA , 4–5 kHz) between a small gold detecting electrode and a larger counter electrode [2–4]. While such a small ac current exhibits no adverse effect on the activity, survival and response of cells to diverse stimuli, cells in contact with the small gold detecting electrode act as insulating particles [1–4]. To date, ECIS has been proven as a versatile

and noninvasive tool for real time measurement of changes in the impedance associated with cell behavior [1–4]. Recently, integrin receptors have been implicated in the measured impedance of cells attached on different extracellular matrix (ECM)-coated electrodes [5]. However, the significance of specific integrins contributing to the impedance measurement has not been determined. It is also not clear how impedance measurements by ECIS can be related to the structure–function of integrins.

Integrins represent the major family of receptors for mediating cell interactions with ECM proteins and cellular ligands in other cells [6]. The noncovalent association between the 18α and 8β unique integrin subunits results in the formation of 24 distinct α - β integrin heterodimers that are found expressed on diverse cell types [6,7]. The binding of integrins to ligands has been shown to impact essential cellular functions including survival, growth, differentiation and

* Corresponding author. Tel.: +1-514-496-6175;

fax: +1-514-496-6265.

E-mail address: john.luong@nrc.ca (J.H.T. Luong).

motility in diverse biological systems such as leukocyte recirculation, wound healing and under pathological conditions, tumor metastasis and the development of autoimmune diseases [8–13]. While the $\beta 1$ integrin subunit mediates the critical interactions with diverse cytoskeletal and signaling molecules, the cytoplasmic domain of α integrin subunits confers signaling properties that are unique to individual members of the $\beta 1$ integrin family [14–18]. Studies of mutation of α cytoplasmic domains have revealed their roles in regulating the ligand binding activities and diverse signaling function of integrins [19–22]. Integrin $\alpha 2\beta 1$ functions as a receptor for collagen and laminin [23–25]. The role of $\alpha 2\beta 1$ integrin in cell adhesion and migration as well as in tumor foci formation has been demonstrated both in vitro and in vivo [26,27]. In addition, deletion of the region of $\alpha 2$ cytoplasmic domain immediately before the GFFKR motif results in dysregulated recruitment of the $\alpha 2\beta 1$ mutant to focal adhesions [21].

This study aims to evaluate the significance of $\alpha 2\beta 1$ integrin in the impedance measurement of cells adhered to different ECM substrates in order to assess whether ECIS detects the effects of structural alterations on the adhesive function of $\alpha 2\beta 1$ integrin. To validate the applicability of ECIS, results from impedance measurements were compared with the adhesive function of the previously characterized human rhabdomyosarcoma (RD) transfectant cells expressing the $\alpha 2$ cytoplasmic domain deletion variant (X2C0) or the wildtype $\alpha 2\beta 1$ integrin (X2C2). Cell attachment as indicated by the measured resistance was indirectly confirmed by monitoring electroporation of the plasma membrane of such adherent cells.

2. Experimental

2.1. Materials and chemicals

2.1.1. Monoclonal antibodies and ECM proteins

Ts2/7 (mAb) specific for human $\alpha 1\beta 1$ integrin was a kind gift from Dr. Martin E. Hemler, Harvard Medical School, Boston, MA [28]. Other integrins including $\alpha 2\beta 1$ -specific mAb BHA2.1, $\alpha 3\beta 1$ -specific mAb P1B5, $\alpha 4\beta 1$ -specific mAb 44H6, $\alpha 5\beta 1$ -specific mAb HA5.1, $\alpha 6\beta 1$ -specific mAb MA6 and pan- $\beta 1$ integrin mAb HB1.1 were obtained from Chemicon International (Temecula, CA). Human fibronectin (MW 440 kDa), collagen type I (MW 116–250 kDa) and mouse laminin I (820 kDa) were obtained from Life Technologies (Gaithersburg, MD).

2.2. Cell characterization by flow cytometry

RD transfectant cells expressing the wildtype $\alpha 2\beta 1$ (RDX2C2) and RD cells transfected with only the expression vector pFneo (RDpF) were prepared and described in the previous studies [9,14]. The cDNA of X2C0 constructed by site-directed mutagenesis introducing stop codons imme-

diately before the GFFKR motif [21] is a generous gift from Dr. Martin E. Hemler (Harvard Medical School, Boston, MA). RD transfectant cells expressing the $\alpha 2$ truncation variant (RDX2C0) were prepared by transfection using the Lipofectin reagent (Life Technologies, MD) according to established procedures [9,14]. All transfectant cells were cultured in RPMI 1640 medium supplemented with 10% fetal bovine serum, L-glutamine, antibiotics and 1.0 mg/ml geneticin G418 (Life Technologies, MD). Integrin expression on RD transfectant cells was assessed by indirect immunostaining according to established procedures [26]. Briefly, cells were incubated with the specific mAb for 45 min at 4 °C, washed and then incubated with F(ab)₂ fragments of the appropriate fluorescein-conjugated second antibody (Cedarlane Lab, Hornby, Ont., Canada). All mAbs were used at predetermined saturating concentrations. Results were analyzed and compared with isotype-matched control mAb by using a Becton Dickinson FACScan.

2.3. Cell adhesion assay

Static cell adhesion assays were carried out as described previously [26,29]. Briefly, untreated microtitre plates were coated with collagen, laminin or fibronectin at varying concentrations overnight at 4 °C. A total of 5×10^4 cells labeled with fluorescence dye, (2',7')-bis(carboxyethyl)-5,6-carboxy-fluorescein (Sigma), were added to each well. After a period of 20 min adhesion at 37 °C, nonadherent cells were removed by gentle washing. The levels of bound fluorescence were measured and subtracted from that on BSA-coated wells as background using a Fluorescence Concentrator Analyzer (IDEXX Lab, Westbrook, ME). Cell adhesion was expressed as number of bound cells per mm², based on the fluorescence of 5×10^4 labeled cells, after a subtraction of background fluorescence.

2.4. ECIS instrumentation

The sensing chip (model 8W1E, Applied Biophysics, Troy, NY) consists of eight detecting gold electrodes (0.057 mm²) deposited on the bottom of eight separate wells. A common counter gold electrode (7 mm \times 46 mm) is shared by the eight detector electrodes on the chip with an active area of 2 mm \times 9 mm in each well. These electrodes and pads are thin gold films (50 nm) sputtered on Lexan polycarbonate by photolithography. The ECIS system (Applied Biophysics) has the capability to carry out simultaneous measurement of 16 individual sample wells.

An alternating current (ac) potential is applied to the detecting and counter electrodes at 1.0 V and 4 kHz through a 1 M Ω resistor. Under this operating condition, the attached cells, acting as insulating particles because of their plasma membrane, interfere with the free space immediately above the electrode for current flow. Consequently, the current cannot pass through the insulating cell membrane and has to flow around the cells. The detecting electrode will dominate

the overall impedance in the circuit because of its smaller size compared to the counter electrode. A lock-in amplifier (Model SR830, Stanford Research Systems, Sunnyvale, CA) is connected between the detector and counter electrodes to measure the magnitude and phase of the voltage. Details on the operation, equivalent RC circuit and modification of the ECIS system have been described elsewhere [31]. The capacitance change is less pronounced than the resistance change [1–4,30] and the relationship between the capacitance change and the number of attached cells has not been established [31]. Therefore, only the results related to the resistance change will be presented and discussed here.

2.5. ECIS electroporation

An elevated field module (model 110A, Applied Biophysics) is inserted in the ECIS front panel. When prompted by software, a switch activates the module, setting up the instrument for invasive operations. Depending upon the applied potential and the exposure time selected, these high fields can be used to electroporate or wound the cells. These invasive actions are only directed at the small population of cells in contact with the active gold detecting electrode, and once these incursions are completed, the system returns to its normal mode to monitor the fate of the effector cells.

2.6. Characterization of ECM coating of electrodes

Sodium chloride solution (0.15 M) was prepared with deionized water (16 M Ω cm, Zenon, Burlington, Ont., Canada). Human fibronectin or laminin was dissolved at 0.1 mg/ml whereas collagen was prepared at 0.2 mg/ml. Each well containing a sensing chip was filled with 0.1 ml protein solution for coating the detector electrode. After 1 h of incubation at room temperature, the wells were washed with distilled water. The amount of protein adsorbed on the sensing chip with bare gold film (the JI chip) was evaluated using the BIAcore 1000 surface plasmon resonance (SPR) biosensor (Biacore AB, Uppsala, Sweden).

2.7. ECIS measurement of cell resistance

A volume of 0.2 ml containing 5×10^4 cells in RPMI 1640/1% BSA was added into each well containing the ECM-coated detecting electrode. Impedance measurements were carried out for 5 h at 37 °C and 5% CO₂. Both data acquisition and processing were performed using a software (ECIS8) supplied by Applied Biophysics (Troy, NY). From the impedance value obtained by ECIS, the impedance of the electrode/electrolyte interface with a cell layer or a RC circuit was estimated using the MathCAD program (Version 7, MathSoft, Cambridge, MA). The number of cells attached to the electrode was determined from digital photos taken from an inverted optical

microscope. Each experiment was repeated a minimum of three times. Results were normalized as resistance change per cell $\Delta R_s/N$ (Ω /cell) where N is the number of RD cells that attached and spread on protein-coated gold electrodes.

3. Results and discussion

3.1. Estimation of the coating of ECM proteins on gold electrodes

Prior to the impedance measurement of cells on ECM-coated gold electrodes, we first assessed the levels of ECM protein adsorption on gold. During the adsorption process, protein molecules substitute the space occupied by water and form a monolayer on the gold surface. As the sensing chips of Biacore and ECIS both have 50 nm gold film lithographs, the surface concentration of protein adsorbed on the gold electrodes of ECIS can be inferred from that of Biacore. A resonance angle shift of 0.1° (1000 response units) of the BIAcore SPR biosensor corresponds to 1 ng/mm² adsorbed protein [32].

Results showed that steady state adsorption of collagen, fibronectin and laminin to gold surface was achieved within 30 min; rinsing with water could not remove protein adsorbed on the gold surface. The surface ECM concentrations were estimated to be 0.9, 3.5 and 5.6 ng/mm² for collagen, fibronectin and laminin, respectively. Consequently, the molecular number of these proteins is 2.9×10^9 mm⁻² for collagen, 4.8×10^9 mm⁻² for fibronectin and 4.1×10^9 mm⁻² for laminin.

3.2. $\beta 1$ integrin expression and function in RD transfectant cells

Human rhabdomyosarcoma cells express little if any endogenous $\alpha 2\beta 1$ integrin. Transfection of cDNA of human $\alpha 2$ integrin subunit results in its expression and the resulting RD transfectant cells (RDX2C2) exhibit increased adhesive function on collagen and laminin substrates [14]. In vivo, $\alpha 2\beta 1$ integrin expression mediates postextravasation cell movement, alters cell distribution within the tissues and modulates tumor formation of RD cells in the lungs and the liver [26,27]. It has been established that $\alpha 2$ cytoplasmic domain plays a major role in the signaling function of $\alpha 2\beta 1$ integrin including the induction of metalloproteinase-1, collagen synthesis as well as activation of p38 MAPK and Rho GTPases [16,18,33,34]. In addition, $\alpha 2\beta 1$ mutant with deletion of the portion of $\alpha 2$ cytoplasmic domain immediately before the GFFKR motif exhibits a major reduction in adhesive function and dysregulated recruitment to focal adhesions [35]. In this study, immunostaining by binding of BHA2.1 to the extracellular region of $\alpha 2\beta 1$ confirmed that wildtype $\alpha 2\beta 1$ (X2C2) and its $\alpha 2$ cytoplasmic domain deletion variant (X2C0) were expressed at comparable levels on

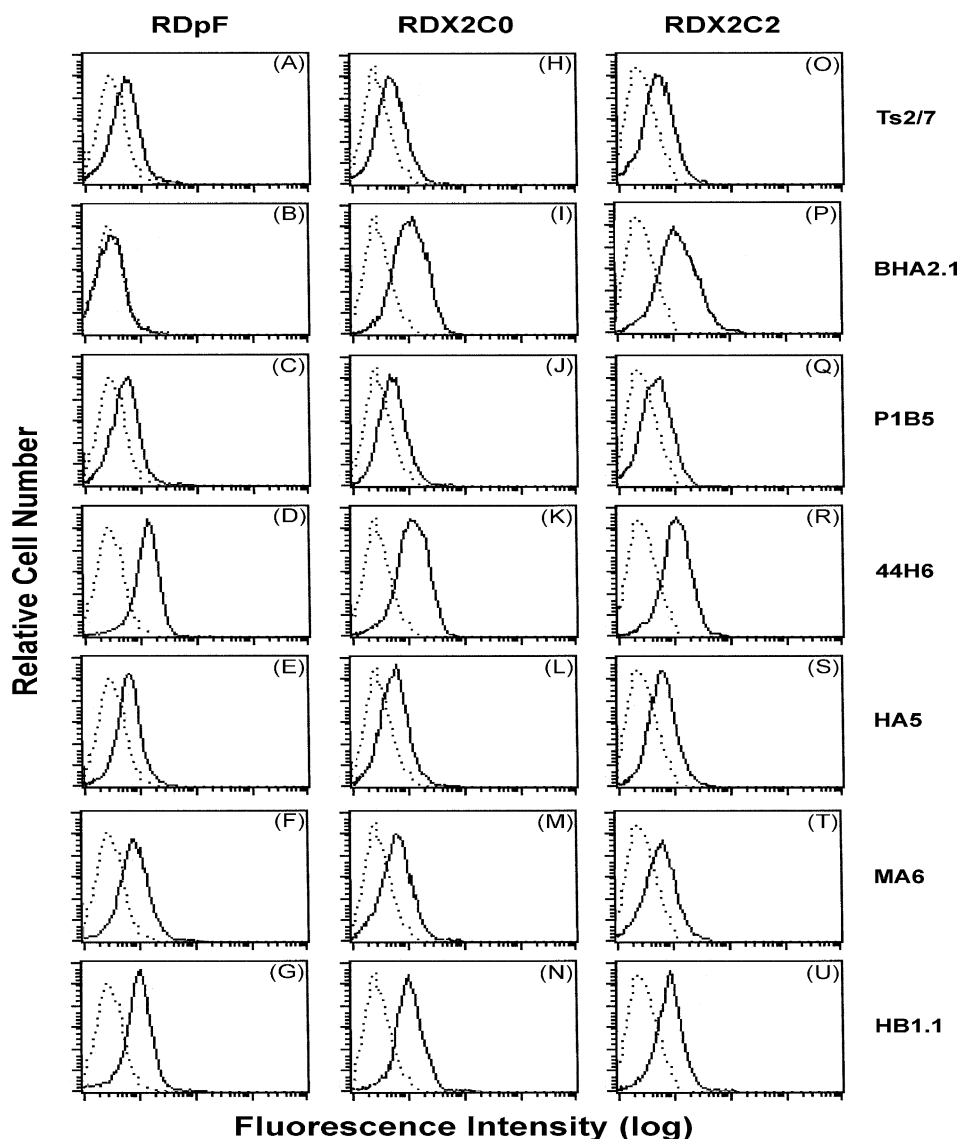


Fig. 1. Expression of $\beta 1$ integrins, $\alpha 1\beta 1$ to $\alpha 6\beta 1$, on RD transfectant cells. The expression of $\beta 1$ integrins was determined by flow cytometry using specific mAbs to the various $\beta 1$ integrins (solid lines). Results were compared with immunostaining using the corresponding isotype-matched control mAbs (dotted lines). The data indicated that expression of $\alpha 2\beta 1$ integrin on RD transfectant cells exhibited no significant effects on the expression of endogenous $\alpha 1\beta 1$, $\alpha 4\beta 1$, $\alpha 5\beta 1$ and $\alpha 6\beta 1$ integrins.

RDX2C2 and RDX2C0 cells, respectively (Fig. 1 I and P). However, mock transfectant RDpF cells exhibited little if any expression of $\alpha 2\beta 1$ integrins. In addition, all three RD transfectant cells were similar in the levels of their expression of endogenous $\alpha 1\beta 1$, $\alpha 4\beta 1$, $\alpha 5\beta 1$ and $\alpha 6\beta 1$ integrins (Fig. 1).

3.3. ECIS assessment of $\alpha 2\beta 1$ integrin-mediated adhesive function on collagen and laminin

Expression of $\alpha 2\beta 1$ integrin enhanced RD transfectant cell adhesion on both collagen and laminin substrates; thus, on both ECM substrates, the levels of adhesion of RDX2C2 cells were greater than RDX2C0 and RDpF cells (Fig. 2A). On collagen, we consistently observed slightly higher levels

of adhesion of RDX2C0 cells than RDpF cells though the difference did not achieve statistical significance. In comparison, RDX2C0 and RDpF were similar in their adhesive function on laminin (Fig. 2B). Such results are consistent with previous studies showing that $\alpha 2$ cytoplasmic domain plays a critical role in $\alpha 2\beta 1$ -mediated cell adhesion on ECM substrates [21].

ECIS data revealed gradual increases in resistance starting at approximately 30 min with steady state resistance achieved in approximately 60 min, after the addition of RD transfectant cells (Figs. 3 and 4). This accounted for the elapsed time required for cell sedimentation, establishment of cell contact and spreading on the ECM-coated gold electrodes. In comparison to RDpF cells, expression of functional $\alpha 2\beta 1$ integrin resulted in increases in the steady state

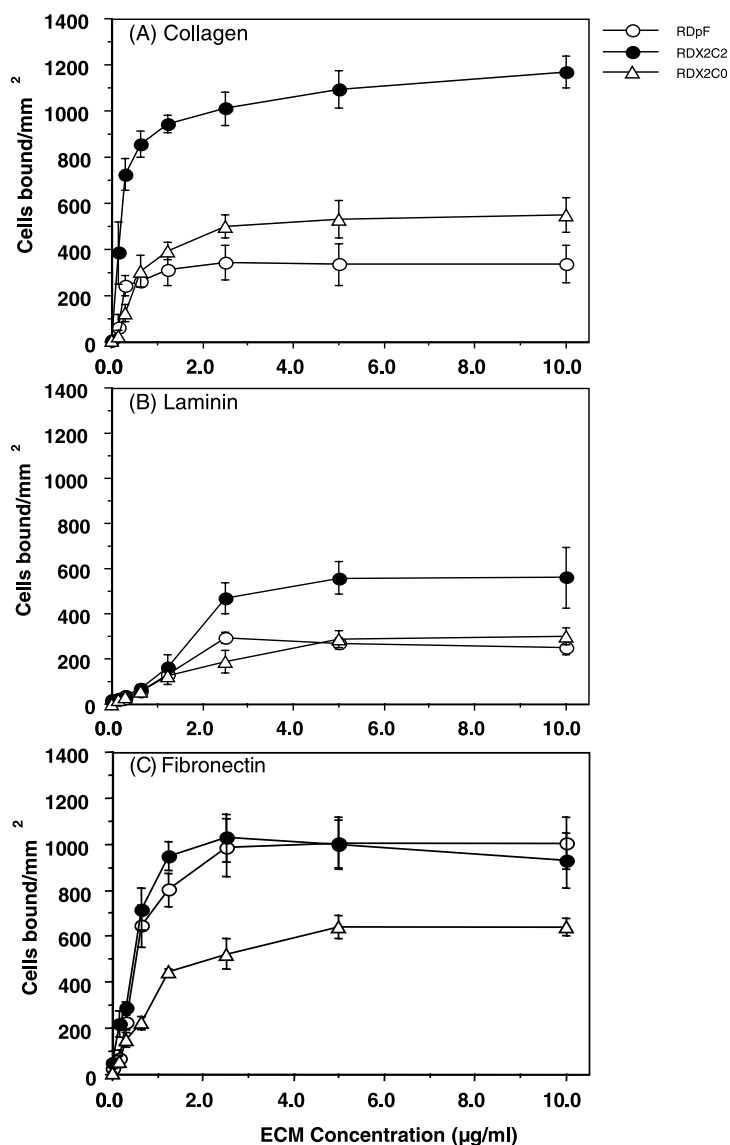


Fig. 2. Adhesion properties of RD transfectant cells for ECM protein substrates. RD transfectant cells (RDpF, RDX2C0 and RDX2C2) were compared for their adhesion to wells coated with varying concentrations of collagen (A), laminin (B) and fibronectin (C). The data showed that on collagen and laminin substrates, X2C0 exhibited little if any adhesive function; whereas on fibronectin, X2C0 reduced RD transfectant cell adhesion to fibronectin. Mean values and S.D.s are shown.

resistance of RDX2C2 cells on both collagen (Fig. 3) and laminin substrates (Fig. 4). Previously, we proposed that $\alpha 2\beta 1$ integrin mediates cell interaction with collagen more efficiently than with laminin [27]. In this study, similar behavior was also observed for collagen-coated electrodes, the resistance measured with RDX2C2 cells ($34.5 \pm 5.2 \Omega/\text{cell}$) was about five-fold greater than that with RDpF cells ($6.5 \pm 0.8 \Omega/\text{cell}$). On laminin-coated electrodes, the resistance measurement for RDX2C2 ($71 \pm 4 \Omega/\text{cell}$) was only twice of RDpF cells ($37 \pm 4 \Omega/\text{cell}$). In addition, ECIS readily detected the effects of $\alpha 2$ cytoplasmic domain deletion on cell adhesion. Thus, on collagen, the resistance measured for RDX2C0 cells ($16 \pm 2 \Omega/\text{cell}$) was intermediate to those of RDpF and RDX2C2 cells (Fig. 3); whereas, on

laminin coating gold, the resistance measured for RDX2C0 cells ($38 \pm 4 \Omega/\text{cell}$) was comparable to that of RDpF cells ($37 \pm 4 \Omega/\text{cell}$) as shown in Fig. 4. The results show that $\alpha 2\beta 1$ integrin plays a major role in the resistance measurement of RD transfectant cells, and ECIS measurement of resistance is closely associated with the adhesive function of $\alpha 2\beta 1$ integrin.

3.4. The effects of $\alpha 2$ cytoplasmic domain deletion on cell interaction with fibronectin

Integrin $\alpha 2\beta 1$ binds collagen and laminin but not fibronectin. Thus, as expected, RDX2C2 and RDpF cells exhibited comparable levels of adhesion to fibronectin

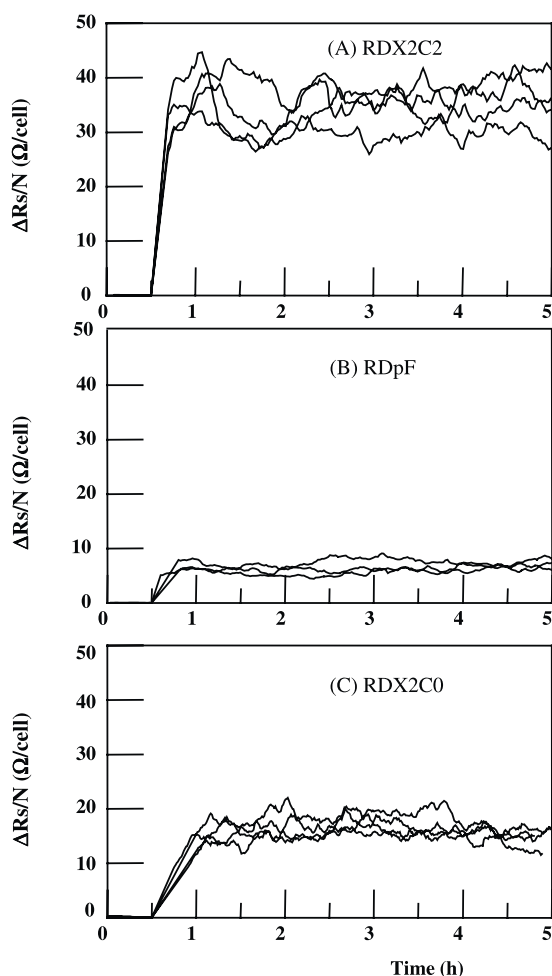


Fig. 3. The resistance change expressed as $\Delta R_s/N$ (Ω/cell) obtained for RD transfectant cells on collagen-coated gold electrodes during the course of the experiment. N is the total number of cells attached on the detecting gold electrode ($250\ \mu\text{m}$ in diameter), precoated with $0.10\ \text{ml}$ of collagen ($200\ \mu\text{g}/\text{ml}$). Other details are in Section 2.1.

substrates (Fig. 2C). It has been shown that deletion of $\alpha 2$ cytoplasmic domain results in ligand-independent recruitment of X2C0 to focal adhesion complexes [21]. Thus, X2C0 has been found in focal adhesions of cells on fibronectin substrate. RDX2C0 cells exhibited reduced levels of adhesion to fibronectin in comparison to RDpF and RDX2C2 cells (Fig. 2C). Adhesion to fibronectin was most likely mediated by endogenous fibronectin receptors, $\alpha 4\beta 1$ and $\alpha 5\beta 1$ integrins, expressed on RD transfectant cells (Fig. 1). Dysregulated redistribution of X2C0 might interfere with the organized formation of focal adhesion complexes and reduce $\alpha 4\beta 1/\alpha 5\beta 1$ integrin function in mediating the adhesion of RD transfectant cells to fibronectin.

ECIS revealed corresponding changes in resistance measurements among RD transfectant cells. Resistance measurements in the presence of RDpF and RDX2C2 cells were similar yielding 89 ± 7 and $85 \pm 5\ \Omega/\text{cell}$, respectively (Fig. 5A–C). Therefore, expression of wildtype func-

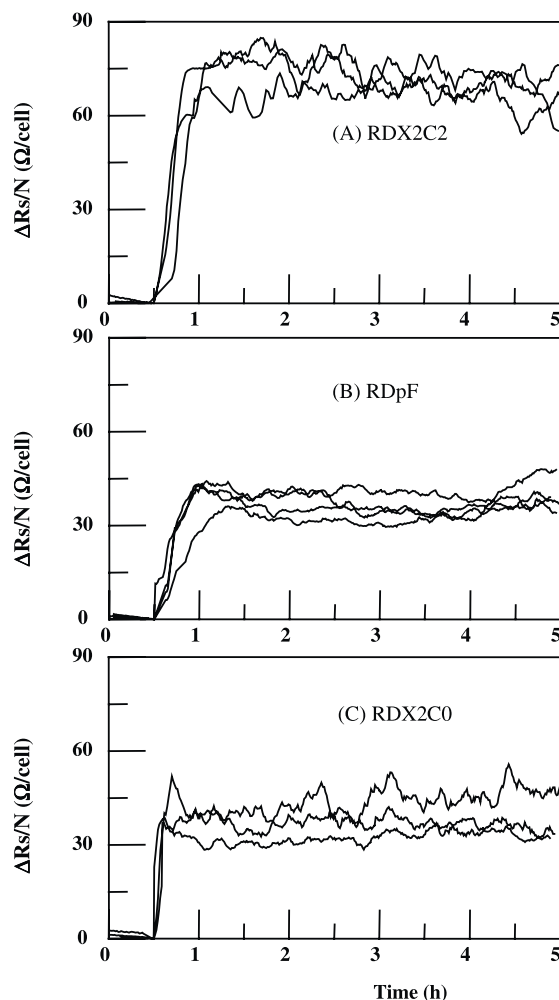


Fig. 4. The resistance change expressed as $\Delta R_s/N$ (Ω/cell) obtained for RD transfectant cells on laminin-coated gold electrodes during the course of the experiment. The detecting gold electrode ($250\ \mu\text{m}$ diameter) was precoated with $0.10\ \text{ml}$ of laminin ($100\ \mu\text{g}/\text{ml}$).

tional $\alpha 2\beta 1$ integrin exhibited no effect on resistance measurements of cells on fibronectin. In contrast, inappropriate recruitment of X2C0 to focal adhesion complexes reduced the insulation properties of RD transfectant cells on fibronectin-coated electrodes; thus, the resistance measured with RDX2C0 cells ($60 \pm 4\ \Omega/\text{cell}$, $n = 7$) was significantly lower than those of RDpF and RDX2C2 cells ($P > 0.05$) (Fig. 5B). Such results thus indicated that all three RD transfectant cells attached more tightly to the electrodes coated with fibronectin than laminin or collagen.

An intriguing feature in the measured resistance was the voltage fluctuation, which was always associated with living cells and persisted even if the cell layer became fully confluent. This behavior is attributed to vertical motions or micromotions of the cells [14], a vertical change in cell morphology that affects changes in the height of the narrow channels, i.e., the transcellular resistance of the layer (resistance under cell).

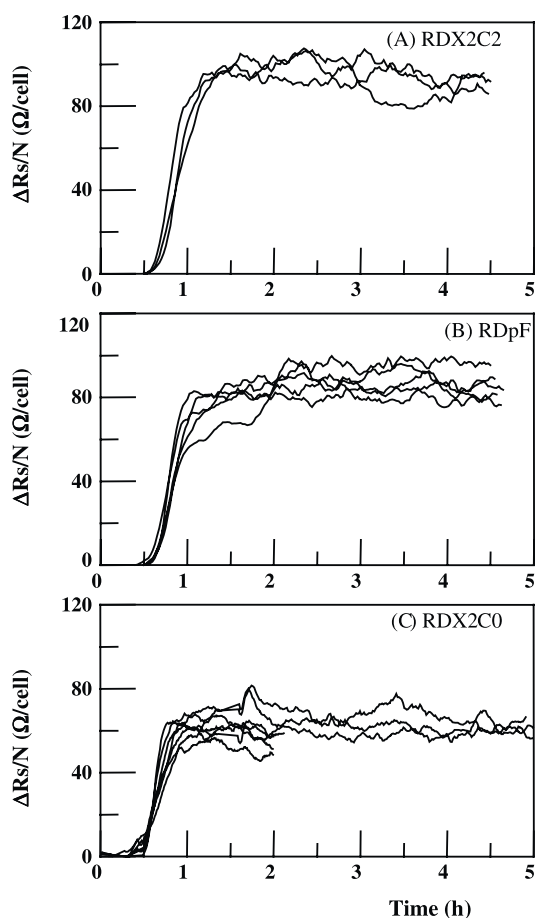


Fig. 5. The resistance change expressed as $\Delta R_s/N$ (Ω/cell) obtained for RD transfectant cells on fibronectin-coated gold electrodes during the course of the experiment. For RDX2C0, some experiments were conducted within only 2 h to reconfirm the value of $\Delta R_s/N$ (Ω/cell) obtained from some other experiments. The detecting gold electrode ($250\ \mu\text{m}$ in diameter) was precoated with 0.10 ml of fibronectin ($100\ \mu\text{g}/\text{ml}$).

3.5. Monitoring electroporation in the plasma membrane

Pore formation occurs when the transmembrane potential ($\sim 60\text{--}100\ \text{mV}$) is raised to $\sim 1\ \text{V}$ and the pores reseal soon after the high field is removed [36–38]. Above this threshold level, irreversible damage takes place, culminating in cell death. Therefore, cell attachment as reflected by the resistance measured could be indirectly verified by monitoring electroporation in the plasma membrane of RD adherent cells. When a RD cell layer was shocked with an applied electric pulse (1–1.5 V for 0.5 s), the resistance decreased considerably owing to pore formation; the tighter the attachment, the larger the drop. As pores started resealing, the resistance recovered but took several hours to attain a value close to the initial resistance before electric shock. Cell recovery, however, was not observed when the applied potential was above 2 V, an indication of irreversible membrane rupture. The fluctuation in the measured resistance ceased when the cells were exposed to

high field (data not shown). Such killed cell data supported the biological nature of the fluctuation, a unique feature of viable and attached cells as detected by ECIS. For typical values of the cell-covered electrode, precoated with fibronectin, the voltage drop across the cell membrane was 60–65% of the applied voltage with the remaining part being distributed over the electrode interface, the solution resistance, and the external resistors. Therefore, when a 2 V signal was applied to the tissue well, it was estimated that $\sim 1.2\ \text{V}$ was across the cell membrane. It was also somewhat difficult to characterize electroporation of RD cells on collagen and laminin as the cells did not attach and spread efficiently on the gold electrode. Microscopic examination also confirmed that there was no migration of neighboring cells into the electroporated area to replace their effector cohorts.

On fibronectin, expression of $\alpha 2\beta 1$ altered both the response and subsequent recovery of RD transfectant cells upon application of 1.5 V (Fig. 6). For RDX2C2, the measured resistance displayed three distinct stages: a rapid initial decrease, a slower secondary decrease and a strong recovery over a long period of time (over 15 h). The recovery was 80% of the initial resistance before electric shock. The initial drop in resistance observed with RDpF was similar to that of RDX2C2, as expected from the resistance measurements for these two cell lines. In principle, if the degree of cell attachment or confluency of two cell layers is similar, their initial response to pulsation will be somewhat identical. However, unlike RDX2C2, there was no secondary decrease in resistance after pulsation and the degree of cell recovery was noticeably weaker, an indication of alteration in membrane permeability. Of interest was the drop in resistance immediately after pulsation observed for RDX2C0, which was smaller than the level observed with RDX2C2 or RDpF. As already demonstrated from resistance measurements, the attachment of RDX2C0 to fibronectin was noticeably weaker than either RDpF or RDX2C2. Therefore, when the potential was applied at 1.5 V, the potential across the RDX2C0 cell layer was not the same as the value attained for RDpF or RDX2C2 cells ($\sim 0.9\ \text{V}$). Such a difference in transmembrane voltage effected an appreciable difference in the initial drop in resistance of the cell layer, immediately after pulsation. Nevertheless, cell recovery with respect to the resistance measured for RDC2X0 was comparable to that of RDpF.

In summary, our results have firmly validated ECIS for real time assessment of cell adhesion and spreading on ECM substrates. For the first time, using the previously characterized RD transfectant cells, we have demonstrated that $\beta 1$ integrins play a major role in impedance measurements. The observed changes in impedance corresponding to deletion of $\alpha 2$ cytoplasmic domain clearly demonstrated the potential of ECIS for studies of the structure–function of diverse adhesion receptors such as members of the integrin, cadherin, and immunoglobulin superfamily of adhesion molecules.

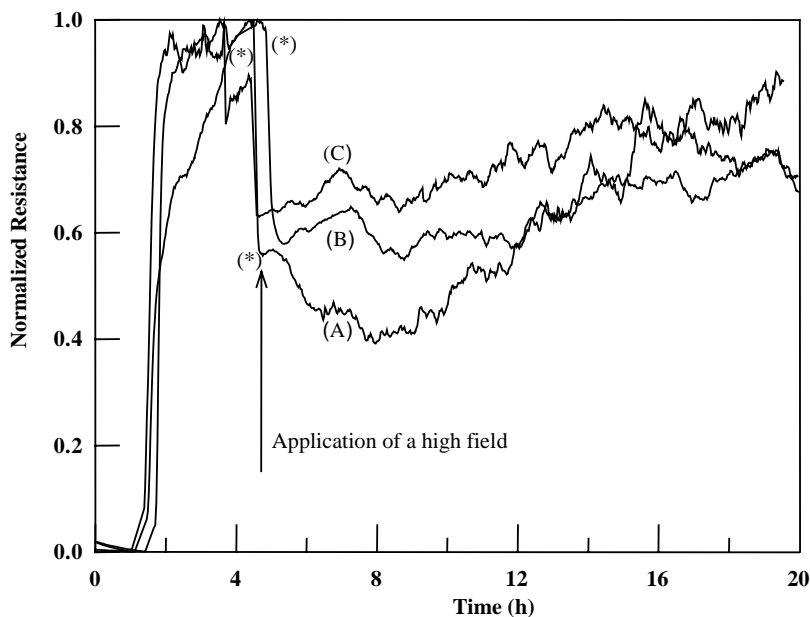


Fig. 6. Observed changes in the measured resistance of a cell-covered electrode due to application of 1.5 V for 0.5 s. Transfectant RD cells were first grown on fibronectin-coated electrodes until steady state was attained. At the point indicated (*), a high field of 1.5 V was applied for 0.5 s and once these incursions were completed, the ECIS system returned to its normal mode of operation to follow the fate of the effector cells. Each curve was averaged from four different electrodes and these results only varied slightly from experiment to experiment. The measured resistance is normalized to the average steady state resistance obtained before electric shock. (A) RDX2C2, (B) RdpF, and (C) RDX2C0.

Acknowledgements

This work was supported in part by grants from Canadian Institute of Health Research and Natural Sciences and Engineering Research Council of Canada.

References

- [1] I. Giaever, C.R. Keese, *Nature* 366 (1993) 591–592.
- [2] I. Giaever, C.R. Keese, *Proc. Natl. Acad. Sci. U.S.A.* 88 (1991) 7896–7900.
- [3] C. Tiruppathi, A.B. Malik, P.J. Del Vecchio, C.R. Keese, I. Giaever, *Proc. Natl. Acad. Sci. U.S.A.* 89 (1992) 7919–7923.
- [4] C.R. Keese, N. Karra, B. Dillon, A.M. Goldberg, I. Giaever, *In Vitro Mol. Toxicol.* 11/2 (1998) 183–192.
- [5] J. Wegener, C.R. Keese, I. Giaever, *Exp. Cell Res.* 259 (2000) 158–166.
- [6] R.O. Hynes, *Cell* 69 (1992) 11–25.
- [7] A. van der Flier, A. Sonnenberg, *Cell Tissue Res.* 305 (2001) 285–298.
- [8] F.G. Giancotti, E. Ruoslahti, *Cell* 60 (1990) 849–859.
- [9] B.M.C. Chan, N. Matsuura, Y. Takada, B.R. Zetter, M.E. Hemler, *Science* 251 (1991) 1600–1602.
- [10] D.S. Tuckwell, S.A. Weston, M.J. Humphries, *Symp. Soc. Exp. Biol.* 47 (1993) 107–136.
- [11] M. de Sousa, *Pathol. Res. Pract.* 190 (1994) 840–850.
- [12] P.A. Rupp, C.D. Little, *Circ. Res.* 89 (2001) 566–572.
- [13] E.A. O’Toole, *Clin. Exp. Dermatol.* 26 (2001) 525–530.
- [14] B.M.C. Chan, P.D. Kassner, J.A. Schiro, H.R. Byers, T.S. Kupper, M.E. Hemler, *Cell* 68 (1992) 1051–1060.
- [15] P.D. Kassner, R. Alon, T.A. Springer, M.E. Hemler, *Mol. Biol. Cell.* 6 (1995) 661–674.
- [16] J. Ivaska, H. Reunanen, J. Westermarck, L. Koivisto, V.-M. Kahari, J. Heino, *J. Cell Biol.* 147 (1999) 401–415.
- [17] K.K. Wary, F. Mainiero, S.J. Isakoff, E.E. Marcantonio, F.G. Giancotti, *Cell* 87 (1996) 733–743.
- [18] P.A. Klekotka, S.A. Santoro, M.M. Zutter, *J. Bio. Chem.* 276 (2001) 9503–9511.
- [19] T.E. O’Toole, Y. Katagiri, R.J. Faull, K. Peter, R. Tamura, V. Quaranta, J.C. Loftus, S.J. Shattil, M.H. Ginsberg, *J. Cell Biol.* 124 (1994) 1047–1059.
- [20] T. Kinashi, K. Katagiri, S. Watanabe, B. Vanhaesebroeck, J. Downward, K. Takatsu, *J. Biol. Chem.* 275 (2000) 22590–22596.
- [21] S. Kawaguchi, J.M. Bergelson, R.W. Finberg, M.E. Hemler, *Mol. Biol. Cell.* 5 (1994) 977–988.
- [22] P.A. Klekotka, S.A. Santoro, H. Wang, M.M. Zutter, *J. Biol. Chem.* 276 (2001) 32353–32361.
- [23] M.J. Elices, M.E. Hemler, *Proc. Natl. Acad. Sci. U.S.A.* 86 (1989) 9906–9910.
- [24] D. Kirchhofer, L.R. Languino, E. Ruoslahti, M.D. Pierschbacher, *J. Biol. Chem.* 265 (1990) 615–618.
- [25] L.R. Languino, K.R. Gehlsen, E. Wayner, W.G. Carter, E. Engvall, E. Ruoslahti, *J. Cell Biol.* 109 (1989) 2455–2462.
- [26] D. Hangan, S. Uniyal, V.L. Morris, I.C. MacDonald, C. von Ballestrem, T. Chau, E.E. Schmidt, A.F. Chambers, A.C. Groom, B.M.C. Chan, *Cancer Res.* 56 (1996) 3142–3149.
- [27] W.-C. Ho, C. Heinemann, D. Hangan, S. Uniyal, V.L. Morris, B.M.C. Chan, *Mol. Biol. Cell.* 8 (1997) 1863–1875.
- [28] M.E. Hemler, J.G. Jacobson, *J. Immunol.* 138 (1987) 2941–2948.
- [29] B.M.C. Chan, M.E. Hemler, *J. Cell Biol.* 120 (1993) 537–543.
- [30] J.H.T. Luong, M. Habibi-Rezaei, J. Meghrou, C. Xiao, K.B. Male, A. Kamen, *Anal. Chem.* 73 (2001) 1844–1848.
- [31] C. Xiao, B. Lachance, G. Sunahara, J.H.T. Luong, *Anal. Chem.* 74 (2002) 1333–1339.
- [32] E. Stenberg, B. Persson, H. Roos, C. Urbaniczky, *J. Colloid Interface Sci.* 143/2 (1991) 513–526.

- [33] O. Langholz, D. Rockel, C. Mauch, E. Kozłowska, H. Bank, T. Krieg, B. Eckes, *J. Cell Biol.* 131 (1995) 1903–1915.
- [34] T. Riikonen, J. Westermarck, L. Koivisto, A. Broberg, V.M. Kahari, J. Heino, *J. Biol. Chem.* 270 (1995) 13548–13552.
- [35] S. Kawaguchi, M.E. Hemler, *J. Biol. Chem.* 268 (1993) 16279–16285.
- [36] E. Neumann, A. E. Sowers, C.A. Jordan, *Electroporation and Electrofusion in Cell Biology*, Plenum Press, New York, 1989.
- [37] D.C. Chang, B.M. Chassey, J.A. Saunders, A.E. Sowers, *Guide to Electroporation and Electrofusion*. Academic Press, San Diego, CA, 1992.
- [38] T.Y. Tsong, *Biophys. J.* 60 (1991) 297–306.